Permeability and Material Characteristics of Vulcanized Latex Film during and following Cyclic Fatigue in a Saline Environment

J. G. DILLON, L. W. SCHROEDER

Food and Drug Administration, Center for Devices and Radiological Health, Office of Science and Technology, Division of Mechanics and Materials Science, Chemistry Group, 12200 Wilkins Ave., Rockville, Maryland 20852

Received 16 February 1996; accepted 14 October 1996

ABSTRACT: The importance of stress or fatigue as a source of latex glove failure has been mentioned in several recent studies, but little work has been done to examine the underlying mechanism of these failures. The present work was undertaken to develop techniques for very early detection of structural changes in glove barriers. This was accomplished by monitoring the ion permeability and electrical properties of vulcanized latex glove material during cyclic fatigue in saline. Alteration in the conductance and capacitance of the membrane during the fatigue cycle showed that catastrophic failure of the material was preceded by deviation in the conductance of the membrane 8–10 min before rupture of the material. Disruption of the material coincided with capacitive "discharge" of and ion transport across the membrane. Follow-up examination by optical (100×) and scanning electron microscopy (SEM) revealed failure of the original fibril network structure surrounding the latex particles. Failure corresponded to processes consistent with repeated stress and rupture of the fibrils responsible for maintaining membrane integrity. Cyclic creep–strain measurements were carried out on the latex glove material. The estimated strain during cyclic fatigue was consistent with use during normal flexing of the glove finger. The fatigue life-time of the glove material was found to be about 2 h. Based on these studies, we conclude that failure of the glove material due to hole formation is preceded by gradual thinning (and weakening) of the membrane in localized regions. This suggests that latex inhomogeneities (defects) are the ultimate cause of failure. These findings confirm the importance of stress in explaining the source of some glove material failures, especially those failures not obviously accompanied by sharp instrument or needle penetrations. The results of the fatigue study emphasize the importance of changing gloves during prolonged use.
 *J Appl Polym Sci **64** 553–566, 1997

Key words: latex; gloves; fatigue; rubber; permeability

INTRODUCTION

Rubber gloves remain one of the most common protective measures against exposure to toxic chemicals, antineoplastic (chemotherapeutic) drugs, and viruses such as HIV.[1] In medical use, breaching the glove barrier via tears or by accidental cuts with surgical instruments has been recognized as a primary means of exposure to these agents.[2] These authors documented the occurence of latex glove tears and sharps injuries among operating room personnel. Interestingly, these researchers observed that the exact cause of

Correspondence to: J. G. Dillon.
 CCC 0021-8995/97/030553-14

glove tears could not be substantiated (by visual confirmation at the time of injury) in about 20% of the reported 249 glove tears and 70 cases thought to be sharp instrument injuries. This number of unidentified sources is probably an underestimate according to the authors.

During use, gloves are repeatedly flexed due to the motions of the fingers and hands while doing various tasks. Colligan and Horstman[3] recognized the significance of induced stress, and studied the permeation of chemotherapeutic drugs under static and flexed conditions. They found the effect of flexing on permeation depended strongly on the quality (thickness) of the glove; surgical (or vinyl) gloves were more resistant than exam latex gloves to permeation. Before conducting their penetration studies, Korniewicz et al.[4] manipulated latex and vinyl gloves according to standardized procedures intended to mimic patient care activities. They reported that holes can be formed in both materials during routine procedures and may be related to the use level. At the highest use level, 7% of latex gloves leaked bacteriophage ϕX 174 virus, indicating an effective hole size greater than 27 nm (0.027 μm). Yoshinari and Yokobori[5] noted the importance of estimating the viscoelastic characteristic properties such as fatigue and creep of membrane materials used in biomedical applications. Surface and interior defects in latex membranes were also implicated in the failure process for glove materials.

The importance of stress or fatigue as a source of latex membrane failure is supported by the work of Goldstein et al.,[6] who measured the transmission of HIV across stressed latex glove material. These authors conclude that repeated stretching of latex gloves causes physical changes that alter permeability and that these changes occur gradually. These researchers also examined the surface of unfatigued and fatigued latex using scanning electron microscopy (SEM) and showed what may be a more porous structure in the fatigued material. Arnold and coauthors[7,8] described the presence of deep holes and pits in latex glove material along with the presence of many embedded particles. Cross sections of the latex glove material showed pores or bubbles throughout. The author believed that while standard test protocols for water or air testing of gloves might find these gloves acceptable, failure could still occur during the stress of normal use and flexion. Thus, it appears that fatigue of the latex glove material and the presence of surface or subsurface defects may play a role in controlling the onset of solute permeation through the glove membrane.

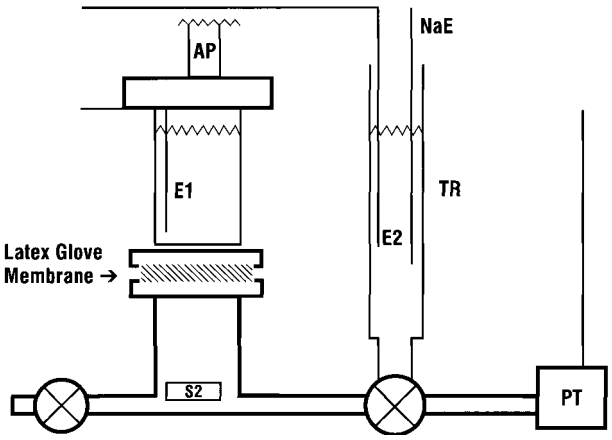

Figure 1 Diagram of latex glove material fatigue apparatus. AP, applied pressure; E1, electrode; S2, stirring bar; NaE, sodium electrode; TR, sidetube; E2, electrode; PT, pressure transducer.

Our research was designed to provide very early detection of catastrophic structural changes in glove barriers rather than changes in steady-state permeability. Careful monitoring in real-time of the electrical property changes in stressed glove materials may provide a better estimate of the underlying mechanism of glove failure. Documentation of an underlying fatigue mechanism would be important in understanding the nature of glove failure where the source of failure is ambiguous. Such changes may be caused by fatigue in the glove material due to repeated flexing.

EXPERIMENTAL

Materials

The gloves were Pharmaseal™ Examination Gloves (Baxter Healthcare, Valencia, CA). All gloves were stored under conditions similar to actual use, i.e., shelf-storage, ambient temperature, unopened boxes, and were tested within 6 months following purchase.

Fatigue Cell and Monitoring Systems

The apparatus used to deform an elastomeric membrane while in contact with various fluids is shown in Figure 1. The fatigue cell is a modified permeation cell (Amicon Corp., Danvers, MA). The lower chamber has been replaced with a

chamber with a graduated side tube and valves for various operations. A disk with a diameter of 2.2 cm is cut from the palm or dorsal side of a latex glove (or any elastomeric barrier) with a die. This disk is clamped between the flanges of the upper and lower chamber and rests against an "O" ring on the lower chamber. Both the upper and lower chambers can be filled with the same fluid or fluids of different composition. When air pressure is applied to the upper chamber, the membrane bulges downward, displacing fluid that then rises in the side tube, TR. The volume of displacement in cm^3 can then be determined. The "O" ring provides some compliance so that the membrane does not fail via the bending at the clamped circumference.

Several monitoring systems are used to measure the change in membrane properties during a fatigue cycle and during the data collection. A pressure transducer (Micro Switch USA) (PT) is attached that produces a voltage proportional to the time varying pressure and allows observation of the pressure waveform during fatigue. The air source is supplied via a pressure regulator at 3–5 psi and the cycle is created by the opening and closing of a solenoid valve (Automatic Switch Co., Florham Park, NJ). The solenoid is operated from a power relay controlled by a signal generator (Hewlett–Packard 3300A, Palo Alto, CA) so that cycle frequencies from 0.01 to 10 Hz can be employed; most experiments used 0.1 Hz (10 s). The use of needle valves on both the input and exit ports of the valve and ballast allows the shaping of the pressure cycle. The pressure cycle is monitored with a Tektronix 324 storage oscilloscope (Tektronix, Beaverton, OR). When the valve is opened to the atmosphere, the membrane returns to the unstretched state at a rate determined by the setting of the exit needle valve. Cycles are counted by a universal counter (Tektronix DC 503) connected to the signal generator.

Shiny platinum electrodes, E1 and E2 in the figure, allow determination of the membrane capacitance and conductance during each fatigue cycle. Saline solutions of sufficient conductivity are employed so that the impedance is due to the membrane. A 1 kHz ac voltage of 1 volt is employed to reduce effects due to an electrical double layer and drifts. A lock-in analyzer (EG & G Princeton Applied Research Model 5208, Princeton, NJ) is used with a very sensitive current-to-voltage converter (I/V) (EG & G Model 181 Preamplifier) to measure the resulting capacitive and conductive current during a pressure cycle and output a voltage proportional to these currents. The capacitive and conductive currents are proportional to the membrane capacitance and conductance.

The capacitance of a membrane is $A\epsilon/l$, where $A = \pi d^2/4$ is the area of the membrane, d is the diameter, l is the thickness, and ϵ is the dielectric constant. If any of these quantities change, then the capacitance changes. During pressurization, the membrane deforms and its area increases. For example, if the membrane deforms to a hemisphere, the new area is twice the original ($\pi d^2/2 \div \pi d^2/4$). During an experiment, ϵ may change because of diffusion of ions into the elastomer, but this affects the membrane in both the original and extended state.

The membrane conductance is given by $A\sigma/l$ where σ is the membrane conductivity (1/resistivity), which is a material property and does not change unless the composition of the membrane is changing. Diffusion of ions into the membrane changes the conductivity, but this affects the membrane in both states and is monitored (see Appendix for more detail regarding validation testing).

Changes in membrane impedance do not always reflect changes in material transport from one side of the membrane to the other. Therefore, we have used sodium ions, Na^+, as a marker. A saline solution containing $1M$ Na^+ is put into the upper chamber and a micromolar Na^+ solution in the lower chamber. The concentration of Na^+ in the lower chamber is monitored during the fatigue experiment with a sodium ion specific combination electrode (Microelectrodes, Inc., Londonderry, NH) (NaE) placed in the side tube. The electrode is connected to a WPI PX-250 pH/Ion Meter (World Precision Instruments, New Haven, CT). Other marker ions with the corresponding ion selective electrodes could be used.

The outputs of the lock-in analyzer, the output from the Na^+ electrode, and the pressure transducer were all supplied to a four-channel computer logging system. Commercially available chromatography software (Chromatographics 3, Perkin–Elmer Corp., Norwalk, CT) was used to simultaneously collect and display the four channels of data. Sigmaplot (Jandel Scientific, San Rafael, CA) was used to plot the data. Preliminary experiments showed that a data collection rate of 12 points/s was needed to depict the pressure, conductance, and capacitance wave forms accu-

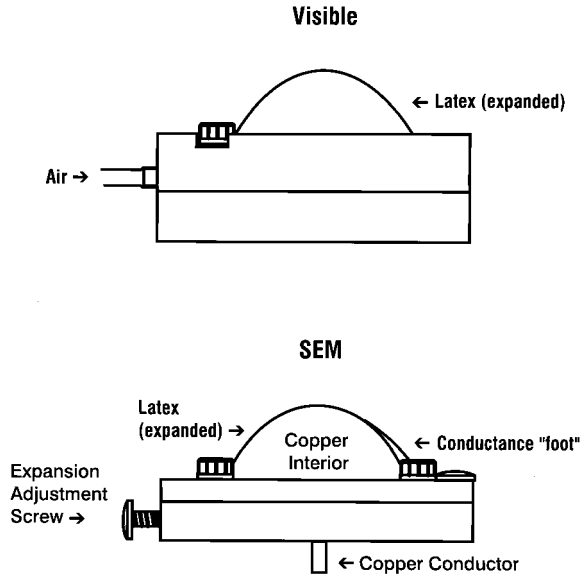

Figure 2 Diagram of apparatus for obtaining visual (100×) (upper) and scanning electron microscopy (SEM) of expanded latex glove material.

rately, while 1 point/s was acceptable for monitoring the sodium ion electrode response.

Optical and Scanning Electron Microscopy (SEM)

An apparatus was constructed so that optical microscopy at various magnifications up to 100× could be carried out on the membrane in both the original and stretched state (Fig. 2, upper). The membrane disk was clamped between a ring and a circular plate. The membrane and the plate then form a small air chamber that can be pressurized. The membrane can then be deformed in the same manner as in the fatigue cell while on a microscope stage. Because the distance from the apex of the membrane to the base plane can be measured, deformation can be controlled. This enabled measurement of the size of defects compared with the nominal membrane area increase for a given deformation. A Zeiss STEMI SU8 optical microscope (Carl Zeiss, Inc., Thornwood, NY) with Schott KL1500 illumination (Schott Corp., Yonkers, NY) was used to photograph the membrane.

Another apparatus was constructed to enable SEM observations of the membrane in the original and stretched states (Fig. 2, lower). The membrane was clamped between two rings; an adjacent copper pressure foot assured conductivity and minimized charging. A copper hemisphere could be inserted through the lower ring to stretch the membrane to various heights above the base plane. This does not stretch the membrane exactly in the same manner as air pressure because the force is only normal to the membrane at the apex. The membrane can be gold coated in this stretched state. Because the membrane is surrounded by conductive material, charging effects in the SEM are reduced. A Technics Hummer V was used to sputter coat the membrane without heat effects followed by examination with a JOEL JSM-5200 scanning electron microscope (JEOL USA, Inc., Peabody, MA).

Membrane Deformation: Nominal Stress and Strain

As mentioned previously, the ratio of the membrane area in normal and unstretched state can be obtained from the ratio of the maximum to minimum capacitances (or capacitive current at constant AC frequency and voltage). A relationship between the membrane deformation and the volume of the displaced fluid can be developed once the geometry of the deformation is determined. The membrane can be considered isotropic, elastic, and homogeneous relative to its dimensions. As shown later, inhomogeneities are of the order of microns in size. The glove membrane is approximately 130 μm thick, giving a ratio of 1/100 of the expected smallest radius of curvature, which is about the disk radius, r, of 1.1 cm. Normally, a ratio of 1/20 or less defines a thin shell.[9] These considerations justify using the Laplace–Young equation to relate the membrane deformation to the pressure difference.[10] In this case, the Laplace–Young equation is:

$$p/T = (1/R_1 + 1/R_2) \qquad (1)$$

where p is pressure difference, T is line tension in membrane (force/length) and R_1 and R_2 are the principal radii of curvature. However, because of cylindrical symmetry, $R_2 = R_1$, and the equation becomes:

$$p/2T = (1/R) \qquad (2)$$

Under these conditions, the profile of the membrane deformation must be a part of a sphere.[11] However, performing the derivation in one dimension and using the axis of revolution passing through the center of the circular membrane to generate the deformation shell is worthwhile. Expressing $1/R$ in cartesion coordinates gives:

$$(d^2y/dx^2)/\{1 + (dy/dx)^2\}^{3/2} = p/2T \quad (3)$$

where y is membrane displacement parallel to the axis of revolution (the y-axis) and x is the radial coordinate. By repeated substitution of variables and using the following boundary conditions: $dy/dx = 0$ @$x = 0$, and $y = 0$ when $x = r$, eq. (3) can be integrated to give:

$$(y + c)^2 = (2T/p)^2 - x^2. \quad (4)$$

This is the equation of a circle with the origin at $(0, -c)$, i.e., on the y axis but below the plane of the undeformed membrane. The radius of the circle, R, is $2T/p$, which decreases as p increases, which is what we expect. Because the y-axis is an axis of revolution, the deformation shell is spherical in nature. R is greater than or equal to r, the radius of the membrane; hence, the shell is only a segment of a sphere, at most a hemisphere. The volume of the displaced fluid under the segment of a sphere is equal to:

$$V = \pi/6(3\ \mathrm{hr}^3 + h^2) \quad (5)$$

where h is the height of the deformed membrane measured at $x = 0$, i.e., the value of y when $x = 0$. By putting eq. (5) into cubic form and with the measured value of V, the value of h can be calculated. Then R can be obtained from the following equation:

$$R = (r^2 + h^2)2h \quad (6)$$

The line tension in the membrane can be calculated as $T = pR/2$. The meridian length, s, is given by the following:

$$s = R\ \sin^{-1}(r/R) \quad (7)$$

The ratio, s/r is the apparent linear strain and $\ln(s/r)$ is the true linear strain. At the full extension corresponding to R, the membrane stress is given by:

$$\sigma = Rp/2l \quad (8)$$

where l is the membrane thickness. For pressurization, the meridial and equatorial (azimuthal) stresses are equal. In our initial experiments, $h = 0.71$r and $R = 1.06$r, giving a spherical section that was close to a hemisphere. For our applied pressure of 5 psi and the dimensions previously given, the membrane stress is 1.55 MPa. This is low, but the meridial strain, s/r is only 1.31 and the true meridial strain is 0.27. This is about what one expects from the linear stress–strain curve of latex.[12–14]

RESULTS AND DISCUSSION

Electrical Property Changes

Figure 3 shows typical electrical property recordings (including pressure and ion transport) from a fatigue experiment carried out over a 2-h period. The intervals displayed are selected to represent electrical properties at critical points in the life of the fatigued membrane and are discussed separately. The conductance and capacitance waveforms are triangular with the return of the membrane to its unstretched state faster than the expansion, although the waveform can be adjusted with the input and exit needle valves.

The values of the capacitance and the conductance in the unstretched state initially increase up to about 20 min then remains nearly constant until the onset of membrane failure. This initial increase, especially in the first several minutes (not shown), is attributed to the diffusion of ions into the latex membrane until equilibrium is reached; this delayed diffusion was also reported earlier by Goldstein et al.[6] and more recently by Aggarwal et al.[14] An increasing concentration of ions in the membrane will increase both the dielectric constant and the conductivity of the membrane. Therefore, the capacitance and conductance of the membrane will increase. This provides an estimate of how long it takes ions to diffuse into the latex membrane while being flexed. If one first equilibrates the membrane in saline overnight, this upward trend is eliminated.

After about 600 cycles (about 2 h), the electrical properties of the membrane show significant change. The first sign of significant change that appears is a subsidiary peak in the conductance waveform at about 122 min (Fig. 3, circle). Close examination of the conductance trace (Fig. 4, left side) shows, in this instance, the appearance of the subsidiary peak at about 117–118 min. The actual onset of this subsidiary peak consistently appears about 9 min before catastrophic rupture of the membrane. This peak occurs immediately before the conductance peak due to the membrane

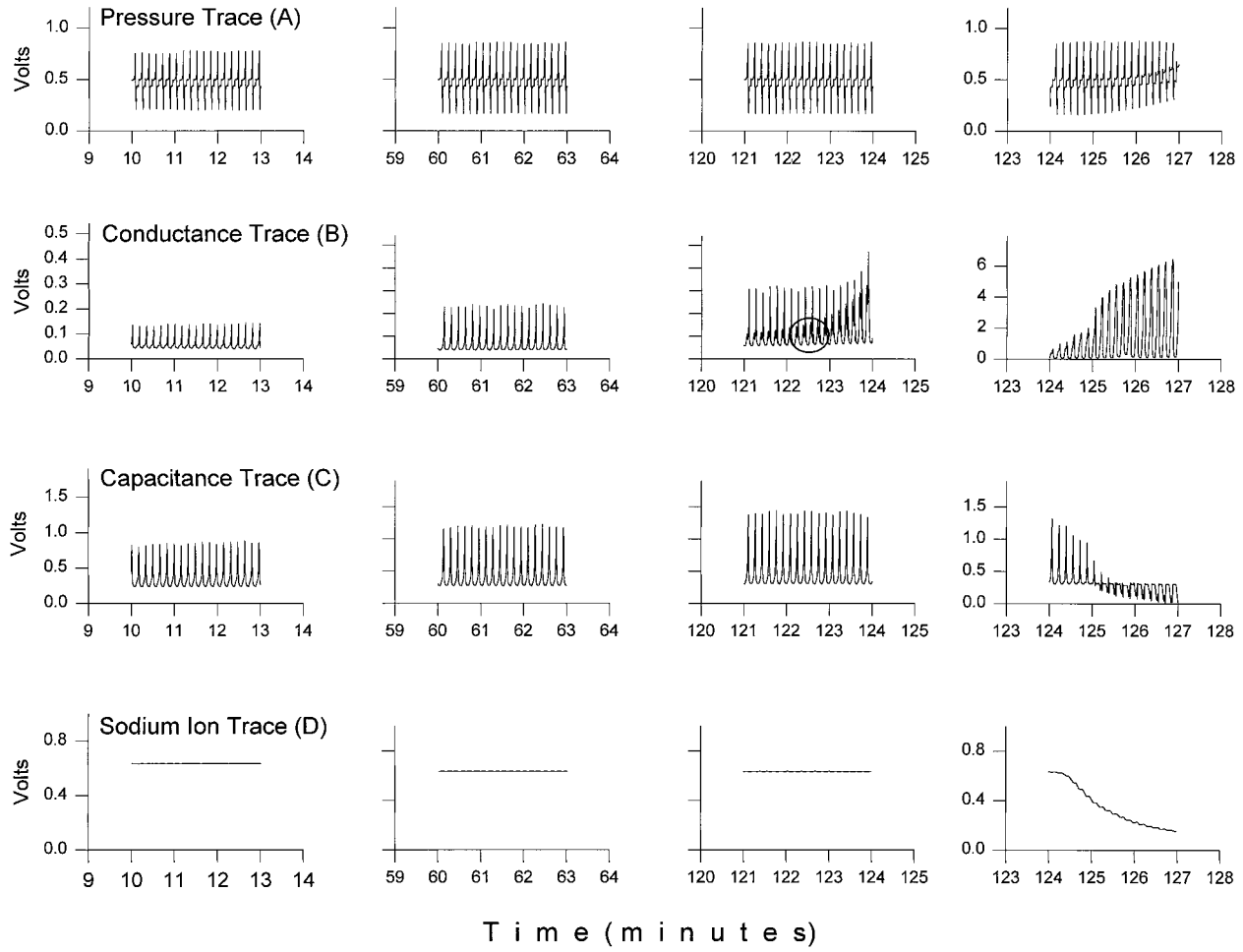

Figure 3 Typical property recordings from a fatigue experiment carried out over a 2-h period on latex glove material. The top trace (trace A) is the pressure waveform variation. The pressure waveform shows several shoulders when the solenoid valves turn on and off. The lower traces show the conductance (B) and capacitance (C) waveforms. The bottom trace (D) monitors the sodium ion concentration in the lower chamber of the fatigue cell. The voltage is inverted in trace D because the electrode produces negative voltages, which tend toward zero, as the sodium concentration increases.

expansion and increases with time. Eventually, this peak is nearly as large as the peak due to expansion and grows even larger (Fig. 4, right side), eventually coalescing with the expansion peak as failure becomes imminent. The corresponding capacitance (Fig. 3, trace C, 124 min) begins to decrease, showing that the latex membrane is not holding a charge, that is, it acts like a "leaky" capacitor. Eventually the capacitor discharges completely during the expansion (Fig. 3, trace C, 125 min) where the capacitive current is zero at the time of maximum membrane expansion. These events can be understood in terms of "hole" or "thin spot" formation in the membrane, both of which we observed optically using our air pressure apparatus. This entire process takes place over a time span of about 8–10 min or about 6–8% of the total time to failure. "Inversion" of the conductance (or capacitance) recordings, as reported by Goldstein et al.,[6] was not observed.

Ion Transport Changes

After 124 min, a significant change in sodium electrode response of about 10 mV is evident over two deformation cycles (20 s) (Fig. 3, trace D, panel 4). The sodium electrode records the change in concentration with time. This abrupt change in

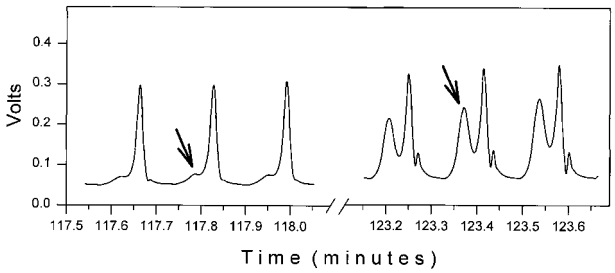

Figure 4 Expanded view of the conductance trace showing the first indication of gradual glove material thinning (and weakening) at about 117.6 min. The newly appearing peak (arrow) increases in size relative to the main conductance peak, indicating increased thinning of the material until rupture occurs.

concentration results from an increased flux of sodium ions through saline filled pores or perhaps "thin spots" in intact latex membrane. This is unsteady-state diffusion because of the creation of pores or "thin spots" by the fatigue process. The time necessary to establish a steady-state diffusion of sodium through the intact membrane is about 20 min, as estimated from the time dependence of the changes in the capacitance early in the experiment. This is supported by the slight shift in sodium electrode response in panel 2 of Trace D from panel 1. In order to assesss ion transport changes that we observed, only an order of magnitude knowledge of the diffusivity of sodium ion in natural rubber is needed. Diffusion coefficients have been measured for Cl^- in isoprene–styrene rubber[15,16] and Ca^{2+} in polychloroprene latexes.[17] Those results suggest a diffusivity of 10^{-7} cm^2/s for Na^+ in latex rubber. This value does give a time to steady state of about 20 min. Hence, we think that the diffusivity of Na^+ in natural rubber is at least 100 times less than the diffusivity in aqueous solution.

The quantity determining the time variation of the flux of sodium ions responsible for the electrode response shown in panel 4 is D/L^2.[18] The derivative of the trace in panel 4 is dc/dt, which is directly proportional to area times the time-varying flux. The time-varying flux can only be the same for a saline filled pore and a "thin spot," if the latter is 1/10 the membrane thickness as then l^2 would be 1/100 smaller and, hence, D/l^2 would be the same. This seems unlikely in that such a "thin spot" will break. The electrode response in panel 4 is roughly consistent with sodium ion diffusion in aqueous filled pores that reaches steady state in a minute or 2. Thicker "thin spots" do not give the same time behavior even if larger areas are postulated because area only scales the magnitude of the sodium flux and does not modify the time behavior. For a "thin spot" of reasonable thickness, i.e., $\frac{1}{2}$ the original thickness, the area of such spots would have to rapidly increase with time in a particular manner. While this is possible, it does not seem very likely; the increased sodium ion transport (panel 4) results, rather, from true pores. This proposal seems reasonable because sodium ion transport into the lower chamber always followed, by a significant amount (here 8 min), changes in the conductance trace. Additionally, little change was noted in the pressure trace (Fig. 3, top) at maximum extension until the time of catastrophic failure, here about 125 min. The pressure decrease, coupled with the concurrent dramatic increase in conductance and capacitive discharge, seems to support the appearance of true pores, as opposed to thin spots. Between 117 and 124 min, the presence of a thin spot or many thin spots seems more likely.

Microscopy of Fatigued Membranes

Microscopy was used to help in interpreting the increase in permeability as detected by the Na^+ electrode and to record the microscopic material changes in the region of membrane failure. Even using 100× magnification, observing any type of "defect" that was obviously a pit or a hole in the unstretched membrane following rupture was often not possible. However, if the membrane was expanded using the air inflation apparatus to a displacement corresponding to that in the fatigue cell, then defects could be observed using 100× magnification. Figure 5 (upper) shows a picture of the unstretched material at 100× magnification. The surface of the material appears smooth and free of obvious holes or other surface defects. The lower picture (Fig. 5) is taken from a fatigued membrane. In contrast to the first picture, many surface defects and possibly holes in the material are visible. A thin fibular-like network structure (arrow) bridging the defects is just visible in some defects or holes.

Subsequently, membrane fatigue experiments were stopped at the time when the subsidiary peak in the conductance waveform was just observable and then the membrane was observed under 100× magnification. In these cases, defects such as pits and cracks were found but no obvious

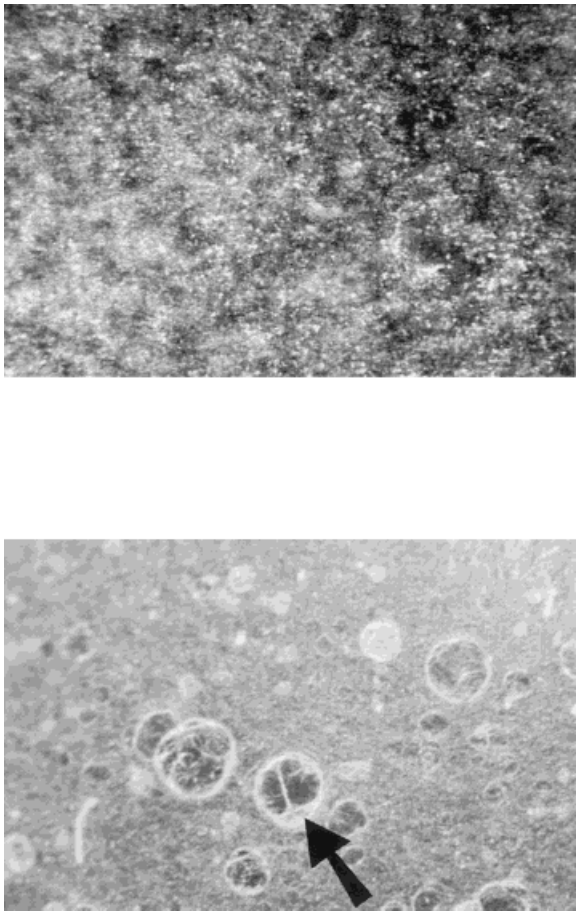

Figure 5 Optical microscopy (100×) of intact latex glove material (upper) and fatigued membrane (below). Note the presence of many surface defects including thinned regions and true pores in the lower picture.

holes were seen in the stretched state. However, if a pit is formed, the thickness of the membrane at that spot is reduced, causing an increase in the conductance. Additionally, the pit membrane may have stretched even more than the nominal extension thus making it thinner. The total conductance is then:

$$A\sigma/l[1 + l/l' \times A'/A] \qquad (9)$$

where the thin spot thickness, l', equals the membrane thickness, l, minus pit depth, and A' is the total area of the pits. The conductance must increase because of the presence of thin spots as all quantities in the second term of eq. (9) are positive.

Figure 6 shows SEM pictures taken of nonfatigued (A–D) and fatigued (E–H) latex glove material. Picture (A) shows the latex material, as received, in an unstretched state. The individual latex particles are clearly visible with no obvious surface pores or other defects. Picture (B) shows the same glove material stretched to a state identical to the maximum stretch achieved in the fatigue cell during normal fatigue conditions. Here, the individual latex particles have been drawn apart revealing a fibril network between the individual latex particles (arrow). This network is more obvious in pictures (C) and (D) taken at higher magnification. The density of the interparticle network in these discontinuous films depends upon polymer interdiffusion, which in turn, depends upon curing conditions.[19,20] The network seems intact in these nonfatigued specimens. Close examination of the surrounding fibrils (D) shows submicron size nodules (arrow) found primarily at the fibril junction points. These nodular filaments may result from plastic deformation of the rubber[21] and represent a higher structural order within the polymer.[22] This yielding process may be a precursor to the ultimate stretching and localized rupture of the rubber during the fatigue process. Pictures (E–F) depict the typical appearance of the latex membrane "holes" in a fatigued glove material. The main difference between the fatigued and nonfatigued membrane is in the fibular network between the latex particles. Picture (E) shows the fragmented nature of the fatigued network with far fewer fibrils reaching out to the latex particle. Picture (F) shows a region where the latex particle is not present but leaves behind a thin network broken in spots and "cracked" in other areas. At higher magnification (G) and (H), the cracking is more obvious. The absence of any surface charging artifact (due to incomplete coating of the latex during SEM sample preparation) in the crack areas provides evidence that the cracks are real and not artifacts due to yielding of the rubber following the coating process. These same cracks were also seen following recoating with a conductive layer, and after allowing the rubber to "age" in an expanded state for 6 days before coating. Close examination of the crack area shows what may be subsurface "necking" of the fibril (Picture H, right-hand fibril). This apparent discontinuation in the fibril may be the result of fracture of a surface "skin" on the cured latex fibril leaving visible an inner core of an uncured latex polymer. It is this inner core of latex that is undergoing the necking often seen in fatigued polymers. The lacy appearance [Fig. 7(A)

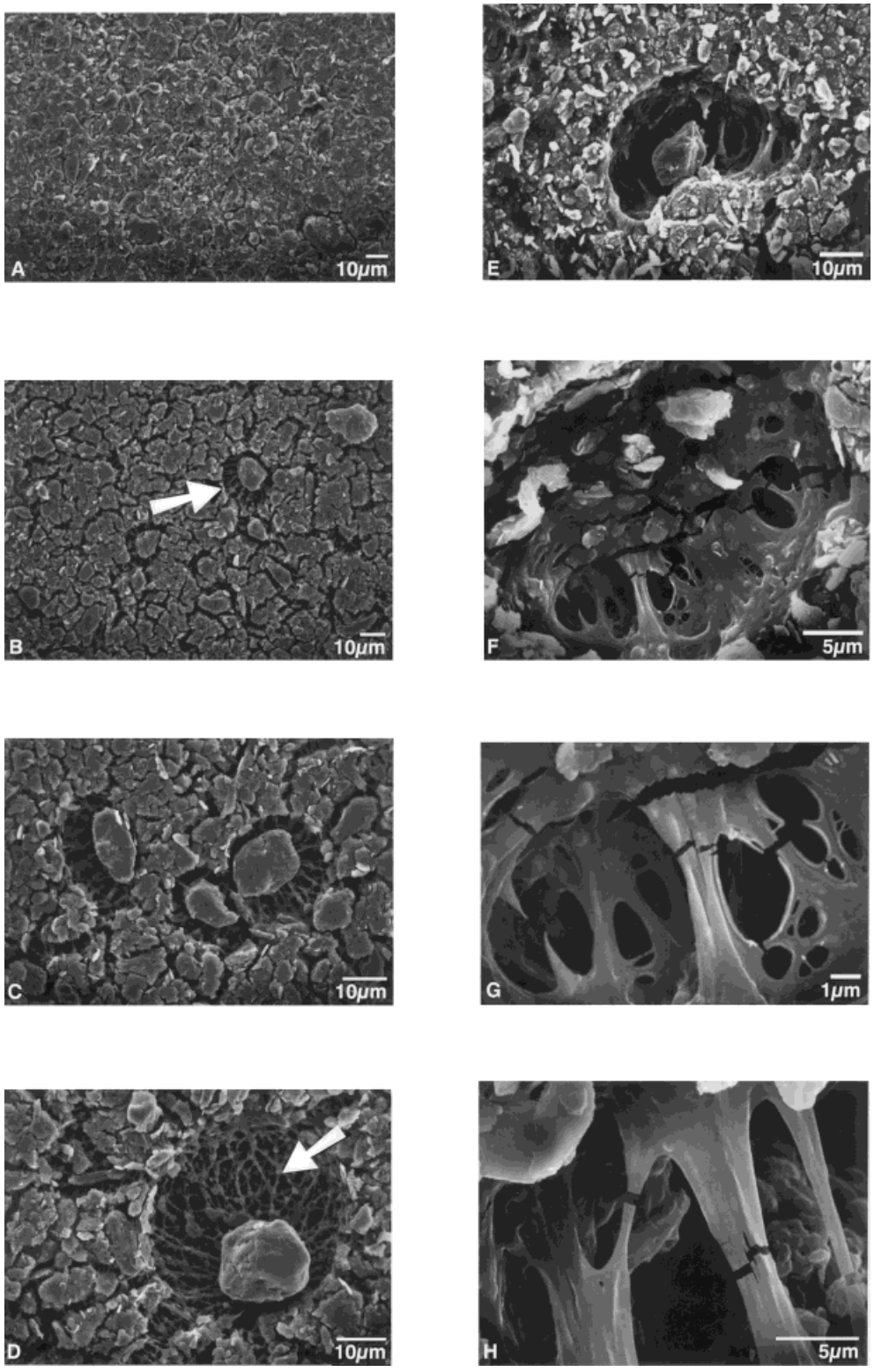

Figure 6 Scanning electron microscopy (SEM) of latex glove material. (A) unfatigued material, no expansion, 750×; (B) unfatigued, expanded, 750×; (C) unfatigued, expanded, 1500×; (D) unfatigued, expanded, 1500×; (E) fatigued, expanded, 1500×; (F) fatigued, expanded, 3500×; (G) fatigued, expanded, 10,000×; (H) fatigued, expanded, 5000×.

and (B)] of the defect region was noted by Bascom[23] and Owen et al.[24] Owen noted the importance of surface area of small voids and filaments in affecting the fracture process. Picture C (Fig. 7) shows a latex particle following fatigue. Present are several fibrils that are in various stages of failure that is cracking, necking down, and rupture. Picture D shows a broken fibril along with a severely cracked fibril. Pictures E and F, taken at much higher magnification, clearly show the presence of what appears to be a stretched surface film surrounding a fractured inner core. The backside of the outer skin can clearly be seen through the fractured inner core of latex in pictures E and F.

While the majority of defects examined by SEM appeared to be caused by stretching and rupture of the fibrils, other surface features are seen (Fig. 7, Picture G). This defect exhibits what might be viscous flow and cavitation—a failure mechanism reported by Bascom[23] for "Viton" fluoroelastomer. In this instance, according to Bascom, polymer chain scission may be the precursor to viscous flow. The author did not rule out the possibility that microcavitation could occur in natural rubber as well. However, because of the long time between the onset of failure and catastrophic rupture (about 8–10 min), the predominant mechanism of failure is likely cyclic stretching followed by rupture.

The fatigue cycle (ca. 0.1 Hz, 10 s) chosen for these experiments likely approximates the cyclic repetition during use of the glove. While this rate is slow by conventional accelerated testing standards, it is relatively fast compared to the "healing" or reptation time (T_r) for natural rubber. Wool et al.[25] have determined the reptation time, T_r, from the self-diffusion coefficient (D) as:

$$T_r = R^2/(3\pi^2 D) \qquad (10)$$

where R^2 is the end-to-end vector given by $R^2 = Mj/M_o C_\infty b^2$. Mj is the molecular weight; M_o is the molecular weight of the monomer; C_∞ is the characteristic ratio for the dimensions of the random coil; and b^2 is the bond length. For natural rubber, the healing time is approximated[25] by

$$T_r = 2.48 \times 10^{-15} M^3 s. \qquad (11)$$

When M (the molecular weight) is 234,000, T_r is 32 s [s represents a constant related to the Brownian motion and displacement of an individual monomer and approximates the square root of t (time) for t less than T_r, the reptation time]. The healing time for rubbers with M of 1,000,000 is about 40 min.[25] Other estimates[26] give even longer times. These long times (relative to actual glove use) likely preclude any "healing" of the latex fibrils during each stretch cycle of only 0.1 Hz, thus predisposing the glove material to early and catastrophic rupture.

The former discussion focused largely on localized defects associated with single latex particles. Occasionally following fatigue of the latex glove material, examination of the surface revealed larger regions or "islands" of particles involved in the fatigue process. Picture H (Fig. 7) shows such a region along with the associated fibular "bridges" spanning the gap between intact membrane and a weaker membrane region. It is this latter region that may dispose the membrane to additional failure.

Failure Curve for Latex Glove Material

The creep of various rubbers under constant tensile load has been studied extensively.[27] However, relatively little work has been carried out under repeated applied loads even though this condition is relevant to many practical applications. To understand the fatigue lifetime of the thin latex membrane under the test conditions, the time to failure for the membrane was plotted vs. the creep–strain (elongation) at failure. The extension was determined from the displaced fluid volume by solving eq. (5) for h and calculating R and s via eqs. (6) and (7). Figure 8 shows the result. The data follow what one would expect in a plot of this type; that is, the lifetime increasing asymptotically as the extension decreases. No fatigue failures occurred in less than 200 cycles, probably because the extensions were not large enough. Larger extensions were not available without altering the membrane geometry and invalidating equations (1–8). The fatigue life-time for the material is about 2 h. This result appears to experimentally support previous investigators'[3,4] conclusions that latex gloves should be changed frequently during use. The estimated strain derived from the volume displacement in the fatigue cell, especially at low strain (0–0.1) is consistent with strain measurements made by Aggarwal[14] on dry and hydrated latex gloves. The scatter in the data may reflect (a) the stochastic nature of fatigue data on natural vulcanized rubber[28,29]; (b) the

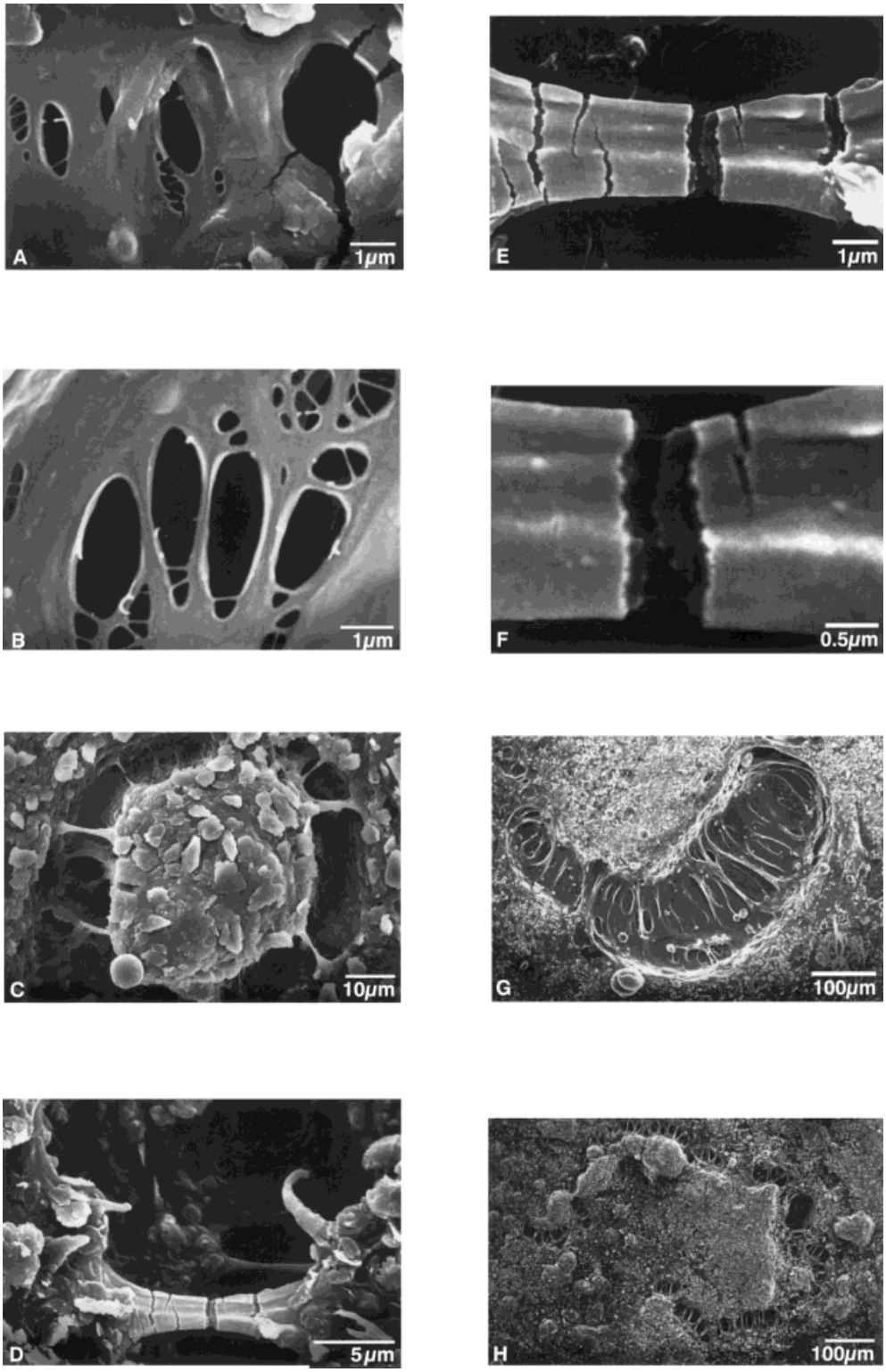

Figure 7 Scanning electron microscopy (SEM) of latex glove material. (A) fatigued material, expanded, 15,000×; (B) fatigued, expanded, 15,000×; (C) fatigued, expanded, 1500×; (D) fatigued, expanded, 5000×; (E) fatigued, expanded, 15,000×; (F) fatigued, expanded, 35,000×; (G) fatigued, expanded, 200×; (H) fatigued, expanded, 150×.

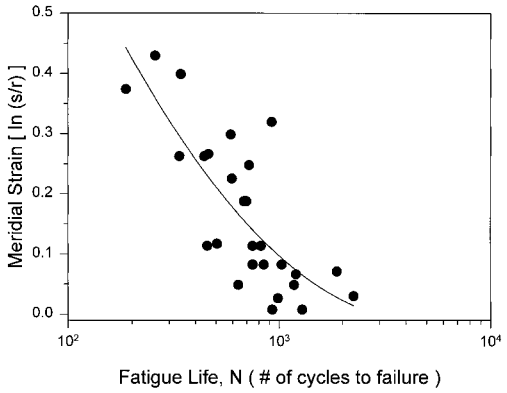

Figure 8 Lifetime curve for latex glove material in saline at ambient temperature.

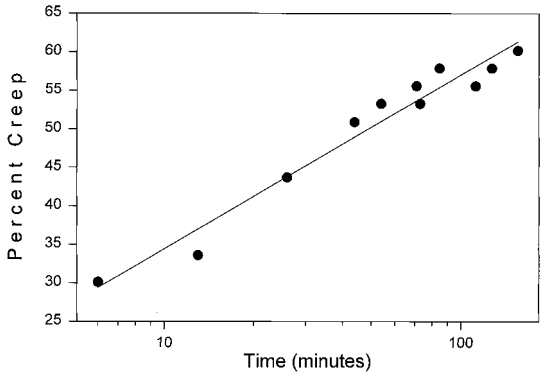

Figure 10 Creep–strain of latex glove material at an initial meridial strain of 0.48.

precision of the test method; or (c) nonhomogeniety in the glove material. We are presently attempting to resolve this question by redesigning the test cell and apparatus to reduce any experimental variability.

Figure 9 shows the creep–strain behavior for the latex glove material at three levels of initial meridial strain. The impact of the initial strain on both the life of the material and the creep are apparent. We examined the effect of strain on cyclic creep by setting three initial levels of meridial strain. The cyclic creep rate is obviously a function of the initial strain. The strains for the nominal 3 mL extension were used to construct a plot of creep vs. time as shown in Figure 10. Creep was defined as $\{s(t)/s(1\ \text{min}) - 1\}$, which eliminates transient effects[27,30] and sets the creep at $t = 1$ min (after six cycles) to zero. This is only a bit different from using the extension at the first cycle ($t = 0$) to normalize the data. Hence, it should be obvious from Figure 10 that the cyclic creep rate is nonlinear for times less than 6 min, but such times are not meaningful in terms of rubber glove usage. From this plot, the creep rate expressed in percent per decade of cycles is about 23%. This creep rate compares well with data reported by Derham and Thomas,[31] who reported cyclic creep rate values of 17–25% for vulcanized latex specimens 1 mm thick. Additional research by these investigators[31] indicated that cyclic creep (as opposed to static creep) produces internal rupture of the rubber network—an observation consistent with our own research results.

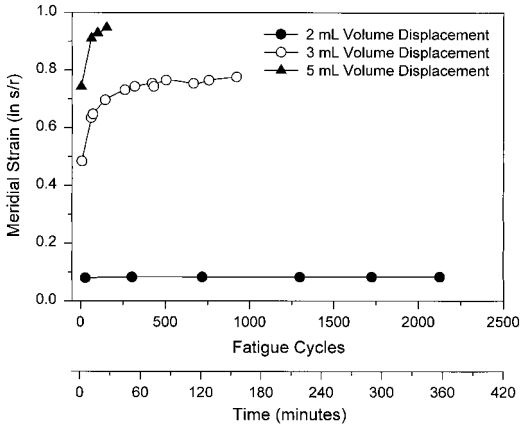

Figure 9 Creep–strain curves for latex glove material at three levels of initial strain.

CONCLUSIONS

A test apparatus has been constructed that allows the monitoring of ion permeability and electrical properties of vulcanized latex glove material during cyclic fatigue in a saline environment. The results of this study show that glove latex failure, under these test conditions, begins nearly 10 min before catastrophic rupture. Sodium ion permeation does not occur until the time of rupture, suggesting that true pores exist only at the time of catastropic failure. Scanning electron microscopy of the fatigued membrane shows stress and rupture of the fibril network surrounding the individual latex particles; the failure of the fibril's outer surface may be ultimately responsible for rupture of the individual fibril. The fatigue lifetime of the latex glove material was found to be about 2 h under stress similar to actual use. The creep rate for the thin latex membrane was approximately 23% per decade of time (or number

of loading cycles). Based on these studies, we conclude that failure of the glove material due to hole formation is preceded by gradual thinning (and weakening) of the membrane in localized regions. This suggests that latex inhomogeneities (defects) are the ultimate cause of failure; that is, the quality of the glove latex may play a role in preventing failure. These findings also confirm the importance of stress, especially cyclic stress, in reducing the glove barrier integrity and may explain the source of some glove material failures, notably those failures not obviously accompanied by sharp instrument or needle penetrations. Lastly, the results of the fatigue study emphasize the importance of periodically changing gloves during prolonged use as the time (about 10 min) from onset of glove failure (fibril rupture) to catastropic failure is only about 10% of the total glove lifetime.

APPENDIX

Validation Tests

The current due to stray capacitance ($\approx$ 1 pF) between the Pt electrodes was only a few nanoamperes, nearly three orders of magnitude below values obtained with membranes. The seal resistance was checked in the following manner. A thick silicone rubber disk (resistivity 10^{15} Ω/cm) was clamped in the cell and the measured resistance was greater than $50M\Omega$, giving a current at least 10 times smaller than the conductive current measured with latex or vinyl membranes. Another experiment involved using a finger from a latex glove with a few cm^3 of saline solution inside and then partially lowered into saline until the capacitive current was similar to that observed with the cell. At this location, the area in common to both saline solutions is comparable to the area of the disk in the permeation cell. Then, the only conductive path from the outside to the inside of the finger is through the latex. The resulting conductive current was similar to that observed for a latex membrane in the permeation cell, confirming the claim that the conductive current measured in the permeation cell does not include a significant contribution from the seal.

The measured capacitance of the latex membrane disk (Pharmaseal latex examination gloves) (d = 2.2 cm, l = 0.13 mm) was 70 pF. This is higher than one would calculate for a disk of pure polyisoprene, but this latex contains salts, processing aids, proteins, etc., and therefore yields a higher dielectric constant than that for natural rubber (2.5–3.0).[32] Expectedly, the measured conductance of the latex membrane is higher than that for polyisoprene.

The authors would like to thank Robert Snyder for conducting the fatigue experiments on the latex glove material.

REFERENCES

1. G. A. Mellström, J. E. Wahlberg, and H. I. Maibach, Eds., *Protective Gloves for Occupational Use,* CRC Press, Inc., Boca Raton, FL, 1994.
2. J. G. Wright, A. J. McGeer, D. Chyatte, and D. F. Ransohoff, *JAMA,* **266,** 1668 (1991).
3. S. A. Colligan and S. W. Horstman, *Appl. Occup. Environ. Hyg.,* **5,** 848 (1990).
4. D. M. Korniewicz, B. E. Laughon, W. H. Cyr, C. D. Lytle, and E. Larson, *J. Clin. Microbiol.,* **28,** 787 (1990).
5. H. Yoshinari and A. T. Yokobori, Jr., *Biomed. Mater. Eng.,* **4,** 333 (1994).
6. A. S. Goldstein, W. Fleming, and K. Stokes, in *Latex as a Barrier Material,* W. F. Regnault, Ed., Food and Drug Administration, Center for Devices and Radiological Health, Rockville, MD, University of Maryland, 1989, p. 175.
7. S. G. Arnold and J. E. Whitman, Jr., *Nature,* **335,** 19 (1988).
8. S. Arnold, *Latex as a Barrier Material,* W. F. Regnault, Ed., Food and Drug Administration, Center for Devices and Radiological Health, Rockville, MD, University of Maryland, 1989, p. 100.
9. A. C. Ugural and S. K. Fenster, *Advanced Strength and Applied Elasticity,* Elsevier, New York, 1981.
10. C. Isenberg, *The Science of Soap Films and Soap Bubbles,* Dover Publications, New York, 1992.
11. H. M. Princen, in *Surface and Colloid Science,* Vol. 2, E. Matijevic, Ed., Wiley-Interscience, New York, 1969, p. 4.
12. J. P. Gerofi and G. A. Shelley, *J. Test. Evaluat.,* **19,** 244 (1991).
13. J. R. Cahoon and A. B. Thornton–Trump, Testing and Stress Analysis of Condoms, Joint HSME/SESA Meeting Hawaii, 1982.
14. M. Aggarwal, T. T. Manson, B. VanMeter, J. G. Thacker, and R. F. Edlich, *J. Long-Term Effects Med. Implants,* **4,** 133 (1994).
15. I. A. Kurmashova, I. V. Gorbunova, and K. M. Gorbunova, *Zhurnal Fizicheskoi Khimii,* **55,** 1899 (1981).

16. I. G. Bogatkov, L. B. Shpaizman, A. L. Iordanskii, and G. E. Zaikov, *Kauchuk I Rezine,* **1,** 24 (1980).
17. C. W. Stewart, Sr., *J. Colloid Interface Sci.,* **43,** 122 (1973).
18. J. Crank, *The Mathematics of Diffusion,* Claredon Press, Oxford, 1975.
19. R.-G. Leonardo, *Makromol. Chem., Macromol. Symp.,* **35/36,** 389 (1990).
20. J. W. Vanderhoff, H. L. Tarkowski, M. C. Jenkins, and E. B. Bradford, *J. Macromol. Chem.,* **1,** 361 (1966).
21. W. D. Bascom, *Rubber Chem. Technol.,* **50,** 327 (1977).
22. J. R. White and E. L. Thomas, *Rubber Chem. Technol.,* **57,** 457 (1984).
23. W. D. Bascom, *Rubber Chem. Technol.,* **50,** 875 (1977).
24. D. R. J. Owen, R. N. Haward, and A. Burbery, *Br. Polym. J.,* **10,** 98 (1978).
25. R. P. Wool, B.-L. Yuan, and O. J. McGarel, *Polym. Eng. Sci.,* **29,** 1340 (1989).
26. C. M. Roland and G. G. A. Bohm, *Macromolecules,* **18,** 1310 (1985).
27. E. R. Praulitis, I. V. F. Viney, and D. C. Wright, in *Elastomers: Criteria for Engineering Design,* C. Hepburn and R. J. W. Reynolds, Eds., Applied Science Publishers Ltd, London, 1979, p. 139.
28. H. H. Kausch and J. G. Williams, in *Encyclopedia of Polymer Science and Technology,* Vol. 7, H. F. Mark, N. M. Bikales, C. G. Overberger, and G. Menges, Eds., Wiley, New York, 1987, p. 328.
29. S. Kawabata and P. J. Blatz, *Rubber Chem. Technol.,* **39,** 923 (1966).
30. K. N. G. Fuller, M. J. Gregory, J. A. Harris, A. H. Muhr, A. D. Roberts, and A. Stevenson, in *Natural Rubber Science and Technology,* A. D. Roberts, Ed., Oxford University Press, New York, 1988, p. 895.
31. C. J. Derham and A. G. Thomas, *Rubber Chem. Technol.,* **50,** 397 (1977).
32. L. A. Wood, in *Polymer Handbook,* J. Brandrup and E. H. Immergut, Eds., Wiley, New York, 1989, p. V8.